Ab initio calculations of the electronic structure and optical properties of ferroelectric tetragonal $BaTiO_3$

1998 J. Phys.: Condens. Matter 10 5645

(http://iopscience.iop.org/0953-8984/10/25/014)

J. Phys.: Condens. Matter **10** (1998) 5645–5655. Printed in the UK PII: S0953-8984(98)88988-1

Ab initio calculations of the electronic structure and optical properties of ferroelectric tetragonal $BaTiO_3$

D Bagayoko, G L Zhao, J D Fan and J T Wang
Department of Physics, Southern University and A&M College, Baton Rouge, LA 70813, USA

Received 4 November 1997, in final form 10 March 1998

Abstract. The electronic structure, charge distribution, effective charge, and charge transfer in ferroelectric tetragonal $BaTiO_3$ are carefully studied using a local density functional potential and a self-consistent *ab initio* LCAO (linear combination of atomic orbitals) method. It is shown that the band gap and low-energy conduction band can be calculated with a reasonable accuracy when the *ab initio* LCAO method is used with an optimum basis set of atomic orbitals. The calculated optical spectrum, band gap, and effective mass of $BaTiO_3$, obtained from the calculated electronic structure, are in good agreement with experimental results.

1. Introduction

Barium titanate ($BaTiO_3$) is one of the most important ferroelectric oxides in electronics applications. It has been widely used in electromechanical actuators and in sensor applications, as a major component of ceramic capacitor dielectrics, and in photo-galvanic devices [1–5]. It is also an important photo-refractive material used for applications in distortion correction, optical limiting, and laser power combining [6]. $BaTiO_3$ undergoes a phase transition from the cubic perovskite structure of the high-temperature paraelectric phase to a ferroelectric tetragonal structure at about 130 °C. Extreme dielectric anomalies accompany this phase transition, which signals the onset of ferroelectricity with a macroscopic polarization along the [001] direction. Upon further cooling, another polymorphic transition occurs at about 0 °C to an orthorhombic phase. This phase transforms to a rhombohedral phase at about −90 °C.

The electronic structure of $BaTiO_3$ has been the subject of some experimental and theoretical studies [1, 2, 7–16]. There has been considerable progress in achieving an understanding of the lattice dynamics and the origin of the ferroelectricity from first-principles total-energy calculations. It has been shown that Ti–O hybridization is essential to the ferroelectric instability in $BaTiO_3$ [10–12]. However, the previously calculated band gap, the conduction band structure, and the effective mass of n-type carriers in the insulating phase are not in agreement with the experimental results. Obtaining a reliable prediction of the band gap in a semiconductor or insulator is a well recognized problem in *ab initio* calculations. These shortcomings, although well known, remain an obstacle in *ab initio* band-gap engineering. There have been some theoretical efforts intended to address these problems [18–20]. However, implementing these theories in practical calculations for materials like $BaTiO_3$ is still a very difficult problem. Instead, in many computations, it is often practical to use some adjustable parameters to get the correct band gaps [17].

In this paper, we explore the problems related to the calculations of the band-gap, low-energy conduction band, and optical spectrum for semiconducting ferroelectric tetragonal

0953-8984/98/255645+11$19.50

$BaTiO_3$. An expanded version of the self-consistent *ab initio* LCAO (linear combination of atomic orbitals) method adopted by the Ames Laboratory (DOE) was used to study the electronic structure of ferroelectric $BaTiO_3$. The charge distribution, effective charge, and charge transfer in $BaTiO_3$ are also calculated using the first-principles electronic wave function. We performed tedious tests and analysis of the role of the atomic orbitals for high-energy excited electronic states in *ab initio* self-consistent computations based on the LCAO method. The optical properties of $BaTiO_3$ were calculated and compared with experimental results.

In the next section, the calculation method is briefly discussed. Section 3 presents the calculated results and compares them with experimental measurements. A short conclusion is given in the last section.

2. The calculation method

In the LCAO method, the atomic wave functions are used as basis functions in which to expand the electronic eigenfunction of a many-atom system. The atomic wave function is constructed from *ab initio* atom calculations and is expressed by a linear combination of Gaussian orbitals (LCGO) in this study. The many-body exchange and correlation interactions of the electron gas are described by density functional theory in a local density approximation [21, 22]. The Ceperley–Alder form of the exchange–correlation potential was used in this calculation [23]. This method has been used by several groups extensively in the study of the electronic structure of various materials [24–29]. Our test calculations and those of others show that the widely used forms of different parametrizations of the local density functional exchange–correlation potential essentially give very similar results for the electronic structure. In the LCAO method, an electronic eigenstate, $\Psi_{\boldsymbol{k}n}(\boldsymbol{r})$, associated with an energy $\epsilon_{\boldsymbol{k}n}$ is expanded as

$$\Psi_{\boldsymbol{k}n}(\boldsymbol{r}) = \sum_{\alpha m} C_{\alpha m}(\boldsymbol{k}n)\phi_{\alpha m}(\boldsymbol{k}, \boldsymbol{r}) \tag{1}$$

where $\boldsymbol{k}$ is a wave vector in the Brillouin zone; $C_{\alpha m}$ is the expansion coefficient of the electron eigenfunction; n is a band index; $\phi_{\alpha m}(\boldsymbol{k}, \boldsymbol{r})$ is a Bloch wave function and is expressed in terms of atomic wave functions as

$$\phi_{\alpha m}(\boldsymbol{k}, \boldsymbol{r}) = \frac{1}{\sqrt{N}} \sum_{l} \mathrm{e}^{\mathrm{i}\boldsymbol{k}\cdot\boldsymbol{R}_l} u_{\alpha m}(\boldsymbol{r} - \boldsymbol{\tau}_m - \boldsymbol{R}_l) \tag{2}$$

where $u_{\alpha m}$ is the atomic wave function for the αth state of the mth atom at the position $\boldsymbol{\tau}_m$; $\boldsymbol{R}_l$ is the translation vector of the lattice.

The effective charge of an atom can be evaluated from the contribution to the coefficients of the electronic eigenfunction in the *ab initio* LCAO method. Then we have

$$\rho(\boldsymbol{r}) = \sum_{m} \rho_m(\boldsymbol{r}) \tag{3}$$

in which

$$\rho_m(\boldsymbol{r}) = \sum_{\boldsymbol{k}n} f_{\boldsymbol{k}n} \sum_{\alpha m' \alpha'} C^*_{\alpha m}(\boldsymbol{k}n) C_{\alpha' m'}(\boldsymbol{k}n) \phi^*_{\alpha m}(\boldsymbol{k}, \boldsymbol{r}) \phi_{\alpha' m'}(\boldsymbol{k}, \boldsymbol{r}) \tag{4}$$

where $\rho_m(\boldsymbol{r})$ is the effective charge density of the mth atom; $f_{\boldsymbol{k}n}$ is the Fermi distribution for the electronic state with an energy $\epsilon_{\boldsymbol{k}n}$ at the $\boldsymbol{k}$-point in the Brillouin zone. A 'nominal temperature' of 400 K in the Fermi distribution was used in the evaluation of the electron population over the energy spectrum. Since the band gap in $BaTiO_3$ is much larger than

this nominal temperature parameter, the Fermi distribution only leads to a full occupation of the valence bands. All of the conduction bands are empty.

The optical spectrum of the dielectric function, $\epsilon(\omega) = \epsilon_1(\omega) + i\epsilon_2(\omega)$, can be calculated once the electronic wave function and energy are known. The imaginary part of the dielectric function $\epsilon_2(\omega)$, from the direct interband transitions, is calculated according to the Kubo–Greenwood formula [29]:

$$\epsilon_2(\omega) = \frac{8\pi^2 e^2}{3m^2\overline{h}\omega^2\Omega} \sum_{\boldsymbol{k}} \sum_{nl} |\langle \Psi_{\boldsymbol{k}n}(\boldsymbol{r})|\boldsymbol{P}|\Psi_{\boldsymbol{k}l}(\boldsymbol{r})\rangle|^2 f_{\boldsymbol{k}l}[1 - f_{\boldsymbol{k}n}]\delta(\epsilon_{\boldsymbol{k}n} - \epsilon_{\boldsymbol{k}l} - \overline{h}\omega) \tag{5}$$

where $\overline{h}\omega$ is the photon energy; Ω is the volume of the unit cell; $\boldsymbol{P}$ is a momentum operator, $\boldsymbol{P} = -i\overline{h}\,\boldsymbol{\nabla}$. The real part of the dielectric function is found from the well known Kramers–Kronig (K–K) relation.

The tetragonal phase of $BaTiO_3$ belongs to the group C_{4v}^1. There are five atoms in a unit cell. The experimentally measured lattice constants, $a_0 = 3.9945$ Å and $c_0 = 4.0335$ Å, were used in the calculation. The atomic positions are: Ba at $(0, 0, 0)$; Ti at $(1/2, 1/2, 1/2 + \delta z(\mathrm{Ti}))$; O_1 at $(1/2, 1/2, \delta z(O_1))$; O_2 at $(0, 1/2, 1/2 + \delta z(O_2))$, and $(1/2, 0, 1/2 + \delta z(O_2))$. Here $\delta z(\mathrm{Ti})$, $\delta z(O_1)$, and $\delta z(O_2)$ are the positional shifts of Ti, O_1, and O_2 along the z-direction (or c-direction). The experimentally measured data are $\delta z(\mathrm{Ti}) = 0.014$, $\delta z(O_1) = -0.025$, $\delta z(O_2) = -0.012$ at room temperature [2, 30, 31]. The shifts of the atoms in the ferroelectric phase destroy the inversion symmetry of the lattice and result in a displacement polarization.

The atomic wave functions in the ionic states of Ba^{2+}, Ti^{4+}, and O^{2-} were constructed from self-consistent *ab initio* atomic calculations. The radial part of the atomic wave functions with an angular momentum l is expanded in terms of Gaussian functions:

$$R_{nl} = r^l \sum_{i=1}^{N} C_i(nl) e^{-\alpha_i r^2} \tag{6}$$

where $N = 23$ for s and p states, and 20 for d states. A set of even-tempered Gaussian exponentials is employed, with a minimum of 0.123 and a maximum of 0.1676×10^6 in atomic units. The charge fitting error using the Gaussian functions in the atomic calculation was about 10^{-4}. Since the deep core states are fully occupied and are inactive chemically in the materials, the charge densities of the deep core states were kept the same as in the free atom. However, the core states of low binding energy were still allowed to fully relax, along with the valence states, in the self-consistent calculation. The frozen-core approximation herein is applied only to deep core states. The atomic orbitals of Ba (4s, 5s, 6s, 4p, 5p, 6p, 4d, 5d), Ti (3s, 4s, 3p, 4p, 3d), and O (2s, 3s, 2p, 3p) were used as an extended valence basis set in the self-consistent LCAO calculation for the electronic structure of $BaTiO_3$. Other atomic states with higher binding energies were treated as deep core states. In this extended valence basis set, Ba(5d, 6p), Ti(4p), and O(3s, 3p) are unoccupied shells in free atoms (ions). Nevertheless, these orbitals are included in the self-consistent LCAO calculation to allow a restructuring of the electronic cloud, including possible polarization. The selection of this basis set is discussed below in the next paragraph. In the *ab initio* calculation of the bulk material, the self-consistent potentials converged to a difference of around 10^{-5} after about 50 iterations. The calculated valence charge error was 0.000 49 for 58 electrons. A mesh of 28 $\boldsymbol{k}$-points, with proper weights in the irreducible Brillouin zone, was used in the self-consistent iterations. A comparison with the results based on 40 $\boldsymbol{k}$-points showed a difference in total energy of only 0.000 02 Ryd. This indicates a satisfactory convergence with respect to the number of $\boldsymbol{k}$-points in the zone.

Table 1. The atomic orbitals used in calculations I to V.

Basis set 0: core-state orbitals in calculations I to V: Ba(1s, 2s, 3s, 2p, 3p, 3d), Ti(1s, 2s, 2p), O(1s)
Basis set for calculation I (set I): set 0 plus Ba(4s, 5s, 6s, 4p, 5p, 4d), Ti(3s, 4s, 3p, 3d), and O(2s, 2p)
Basis set for calculation II (set II): basis set I plus Ba($5d^0$), Ti($4p^0$), and O($3s^0$)
Basis set for calculation III (set III): basis set II plus Ba($6p^0$) and O($3p^0$)
Basis set for calculation IV (set IV): basis set III plus Ti($4d^0$)
Basis set for calculation V (set V): basis set IV plus Ti($5s^0$)

Table 2. The calculated electron energies (in Ryd) at the Γ and X points for the valence and low-energy conduction bands.

Calculation I	Calculation II	Calculation III	Degeneracy
Γ point:			
−0.410	−0.477	−0.513	1
−0.408	−0.475	−0.511	2
−0.306	−0.390	−0.417	2
−0.294	−0.379	−0.406	1
−0.220	−0.314	−0.352	1
−0.211	−0.307	−0.346	2
0.045	−0.096	−0.123	1
0.061	−0.079	−0.107	2
0.133	0.008	−0.021	1
0.150	0.020	−0.011	1
X point:			
−0.509	−0.597	−0.641	1
−0.454	−0.528	−0.552	1
−0.451	−0.525	−0.549	1
−0.387	−0.465	−0.495	1
−0.358	−0.439	−0.470	1
−0.354	−0.433	−0.457	1
−0.341	−0.418	−0.444	1
−0.268	−0.371	−0.404	1
−0.260	−0.364	−0.398	1
0.060	−0.056	−0.084	1
0.135	0.013	−0.049	1
0.138	0.019	−0.045	1
0.143	0.022	−0.016	1
0.251	0.133	0.101	1

In addition to the above general formalism, our calculations employed a new procedure to avoid a spurious effect due to the basis set and the variational approach. This effect arises from the combination of:

(a) the use of larger basis sets to ensure completeness,

(b) the tendency of the Rayleigh–Ritz variational method to lower eigenvalues as the size of the basis set increases, and

(c) the use of the wave functions for the *occupied states*, from one iteration to the next, in reconstructing the charge density and the potential.

Unnecessarily large basis sets directly lead to spuriously low *unoccupied* energy levels strictly on account of the variational method. We avoided these unphysical effects as follows. We performed the calculations with the minimum basis set. We then repeated the calculations with an extended basis set that included orbitals for the lowest-lying unoccupied atomic levels. We compared the occupied energy levels from calculation I and II to check for any significant qualitative (branching) and quantitative (numerical difference) changes. We concluded that the extended basis set had to be preferred to the previous one (the minimum basis). We proceeded similarly, by expanding the basis set, as compared to that of calculation II, to include orbitals for the next-lowest-lying atomic levels. The completely self-consistent calculation III was carried out, and the resulting occupied energy levels were compared to those from calculation II. Qualitative and quantitative differences indicated that the basis set in calculation III had to be preferred. This process was continued with calculations IV and V. The optimum basis set selected for all of the results discussed here is that of calculation III. This selection was based on the fact that calculation IV did not change—qualitatively or quantitatively—the occupied energy levels as compared to the results from calculation III. It did lower some unoccupied energy levels. Calculation V also left the occupied energy levels unchanged even though it led to different unoccupied energy levels as compared to the output of calculation III and that of calculation IV. An essential feature of the results obtained here, with the basis set in calculation III, resides in the fact that they do not suffer from spurious basis-set and variational lowering of the unoccupied energy levels. The atomic orbitals used in calculations I to V are summarized in table 1. The calculated electron energy levels (in Ryd) at the Γ and X points for the valence and low-energy conduction bands are listed in table 2. Table 2 shows the tendency of the Rayleigh–Ritz variational method to lower eigenvalues as the size of the basis set increases.

3. Results

3.1. The electronic structure, band gap, and low-energy conduction band

The calculated electronic band structure of the tetragonal phase of $BaTiO_3$ is shown in figure 1. The zero of the energy was set at the top of the valence band. High-symmetry points in the Brillouin zone include: $\Gamma = (0, 0, 0)$; $Z = (0, 0, \pi/c)$; $X = (\pi/a, 0, 0)$; $M = (\pi/a, \pi/a, 0)$; and $A = (\pi/a, \pi/a, \pi/c)$. The electronic structures of the valence bands, the band gap, and the low-energy conduction bands determine the most important properties of the material in electronic device applications. The calculated valence bands below the Fermi energy agree well with other first-principles studies [10, 12, 14, 16]. Figure 1 shows that the *ab initio* LCAO method yielded an indirect band gap (E_g) of 2.6 eV, quite close to the experimental values of 2.8 to 3.0 eV [1, 2, 4]. There are some experimental complications in determining the exact band gap, including the optical absorption edge tails which extend to several tenths of an eV [1]. Figure 1 shows that the top of the valence band is at point A. There is a strong anisotropy of the effective mass of the holes around the top of the valence band at point A. The calculated effective mass of the holes along the c-direction (or z-direction) is about 7–8 m_0. But the effective mass on the plane perpendicular to the

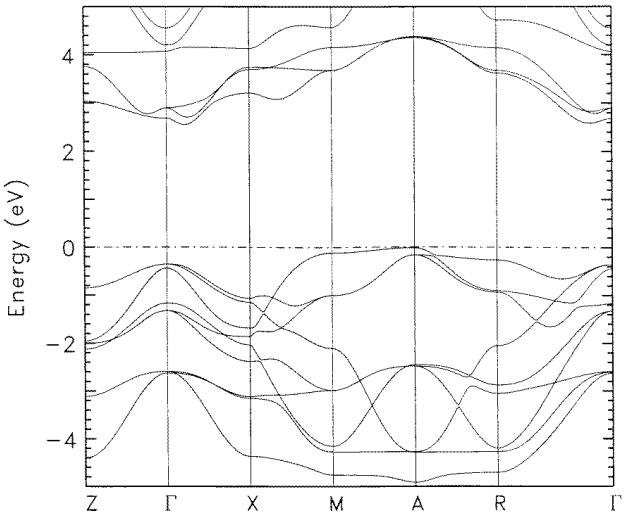

Figure 1. The calculated electronic band structure for ferroelectric tetragonal $BaTiO_3$. The zero of the energy was set at the top of the valence band.

c-direction is only about 1.1–1.3 m_0. This is consistent with the experimental findings of a strong anisotropy in the hole drift mobility in this material. The anisotropy of the hole drift mobility, $\mu_\perp/\mu_\parallel$, may reach a value of about 8 at $T = 90$ °C, and about 19 at 20 °C [32]. The mobility (μ) of the holes is related to the effective mass (m^*) by $\mu = e\tau/m^*$, where τ is the relaxation time. The anisotropy of the effective mass estimated from the experimental data, under the assumption that the effective mass is independent of the temperature and that $\tau_\perp/\tau_\parallel$ is about 1 at $T = 90$°C, is about 8.

The calculated low-energy conduction bands in figure 1 are quite different from those of previous studies. Figure 1 shows that the lowest energy states of the conduction bands are not at the Γ point. There are shallow minima near the Γ point along the [100] and equivalent directions. The electronic structure in figure 1 was calculated using the experimental lattice constants (a_0 and c_0). We further examined whether the positions of the shallow minima in the lowest conduction band depend on the values of the lattice constants a and c. We performed the calculations with one per cent increases in both a_0 and c_0. We repeated the computation twice, the first time with one per cent contraction of both a_0 and c_0, and a two per cent contraction the second time. The calculated electron structures show an increase of the band gap from about 2.5 eV for a/a_0 and c/c_0 at 1.01 to a gap value of about 2.8 eV for a/a_0 and c/c_0 at 0.98. However, the position and the depth of the shallow minimum in the lowest conduction band do not show appreciable change in these three test calculations. The shallow minimum may be smeared by the thermal or static disorder or other impurity effects. The effective mass along the [100] direction may be subject to this smearing effect. For a perfect crystal, the effective mass for n-type carriers in the tetragonal phase of $BaTiO_3$ along the [100] direction is about 1.1–1.3 m_0. The effective mass can be raised to about 1.5 m_0 or higher by the smearing effect. The effective mass along the [001] direction (the c-direction) is much higher than that in the [100] direction and was found to be between 3 m_0 and 4 m_0. The properties calculated from the predicted conduction band agree well with the electron transport measurements for single-domain, n-type, ferroelectric barium titanate in the tetragonal phase [33]. The experimental measurements found a strongly anisotropic

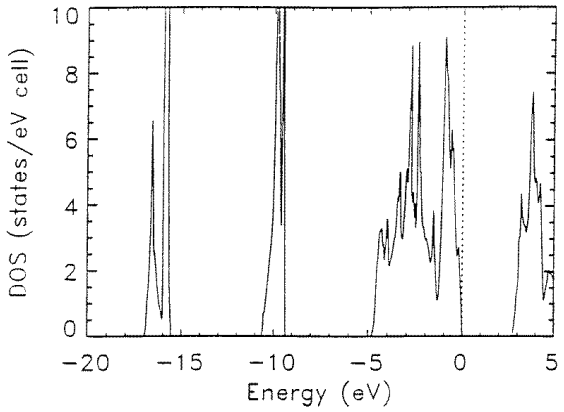

Figure 2. The total density of states (DOS) for ferroelectric tetragonal $BaTiO_3$.

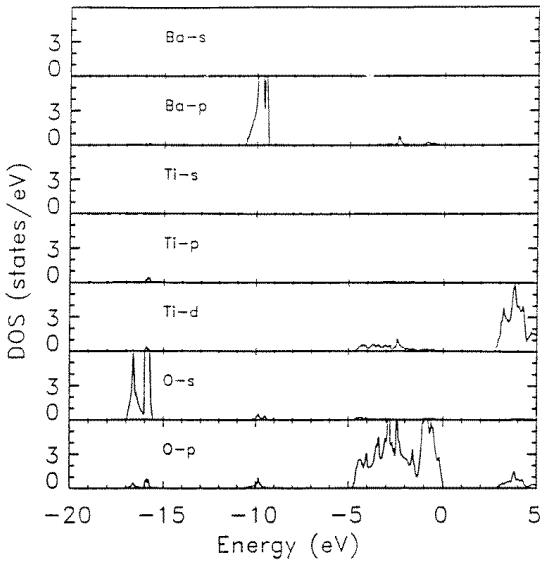

Figure 3. The partial densities of states (PDOS) showing the contributions of Ba, Ti, and O atoms. One Ba, one Ti, and three O atoms from one unit cell of tetragonal $BaTiO_3$ are included in the calculation.

effective mass along the [100] and [001] directions as confirmed by our calculation. A conduction band with a many-valleyed structure was also suggested on the basis of the experimental data [33].

3.2. The electronic density of states and charge distribution

The electron distribution in an energy spectrum is described by the density of states (DOS) and can be measured in photoemission experiments. The total DOS spectrum of tetragonal $BaTiO_3$ is shown in figure 2. The valence and conduction band edges near the Fermi energy are quite sharp. This is consistent with the experimental finding of a relatively

sharp absorption edge in optical measurements for $BaTiO_3$. Another very useful piece of information to examine is the hybridization and charge distribution. The partial densities of states of the Ba, Ti, and O atoms are shown in figure 3, where the low-energy peak at around −17 to −15.5 eV is a contribution mainly from the O 2s states with a small component from Ti p and O p orbitals. The DOS peak at around −10 eV mainly represents the contribution of Ba 5p states which are weakly hybridized with the O s and O p states. Since the wave function of the semi-core state of Ba 5p is quite extended, the intersite overlap of the Ba 5p states and the resulting hybridization with other atomic wave functions lead to an appreciable band dispersion in these electronic states. This type of behaviour is different from the featureless, straight line for the deep core states. The bands below −20 eV are featureless deep core states without appreciable dispersion. The valence states from −4.7 eV up to the Fermi energy are dominated by the O 2p states and strongly hybridized with the Ti 3d states. It should be pointed out that the PDOS spectrum in figure 3 includes one Ti atom, and three O atoms. Therefore, the height of the O 2p DOS peak is much higher than that of the Ti 3d states. There is only a very weak hybridization of the Ba p state with the O 2p state in the valence band.

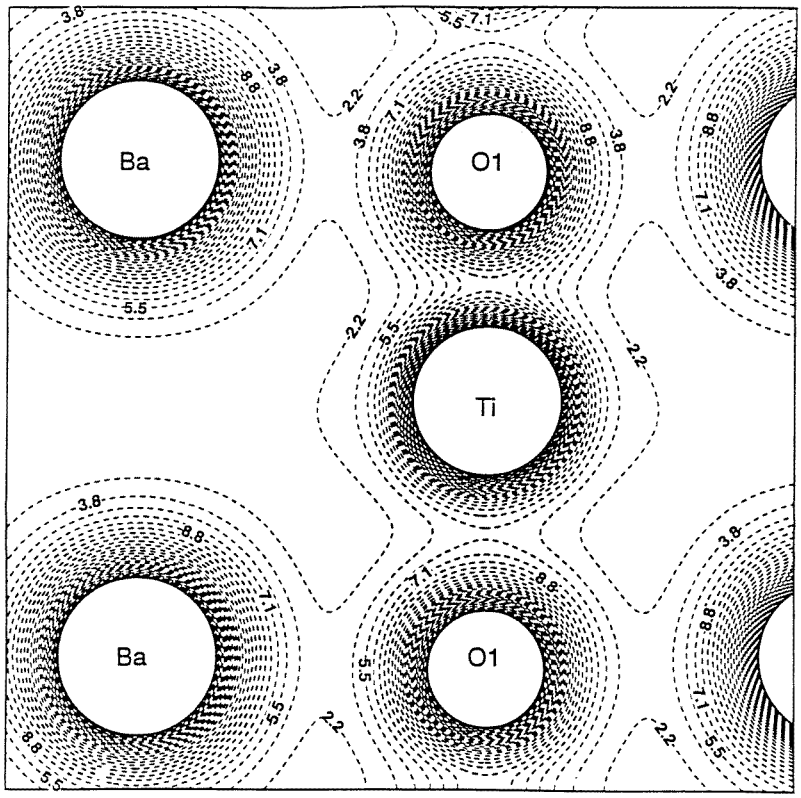

Figure 4. The charge-density map on a (110) plane passing through Ba, Ti, and O1 atoms.

The contribution from the low-energy portion of the conduction band is also shown in figure 3. The major contribution around the conduction band edge is from the Ti 3d states with a small component from the O 2p states. A direct consequence of the electronic structure of $BaTiO_3$ is that the photo-excitation of the electrons from the top of the valence

band to the bottom of the conduction band will have the effect of bringing electrons from the oxygen atoms to the titanium atoms. This will lead to a noticeable change of the effective charge of the Ti and O atoms. The modification of the effective atomic charge then changes the local dipoles and the dielectric properties. The photo-electron process leads to a strong photo-refractive and photo-restrictive behaviour in ferroelectric $BaTiO_3$.

The electron charge density in real space for the tetragonal phase of $BaTiO_3$ is shown in figure 4, where a (110) plane passes through Ti, Ba, and O1 atoms. The unit of the charge density in these diagrams is 10^{-2} electrons/r_0^3, where $r_0 = 0.529\,177$ Å. The high-charge-density region around the nuclear sites has been cut off at a value of 0.5 electrons/r_0^3 in these diagrams, leaving an empty space to represent the atomic cores. From figure 4, it appears that the Ba–O bond is typically ionic. The Ti–O bond has a strong covalent character. This is partly apparent from the noticeable charge distribution at the middle of the Ti–O bond. There is not much bonding charge to link the Ba and O atoms. The atomic size may be estimated from the charge distribution in figure 4. In perovskite $BaTiO_3$, the Ba atoms form a backbone of the lattice. The size of the Ba atoms is much larger than that of Ti and O. It is interesting to see that the size of the oxygen atoms is only slightly larger than that of the titanium atoms. Of course, the determination of the atomic size is largely dependent on how one divides up the electron charge in real space. The charge distributions in figure 4 are consistent with the reported results of Weyrich and Siems [8].

The effective charge of tetragonal $BaTiO_3$ was computed using the calculated electron wave function and equation (4). It was found that each Ba atom lost about 2.0 electrons. The Ti atoms gave away about 2.35 electrons. The O atom gained about 1.45 electrons. The ionic formula for this material may be written as $Ba^{2.0+}Ti^{2.35+}O_3^{1.45-}$. The error in the computation of the charge transfer is estimated as about 15%, much larger than that in the electronic structure calculation, because of the difficulties in the procedure of decomposition of the electronic eigenfunction in the computation of the effective charge. The effective charge calculated from our study is quite close to the results reported by Cohen and Krakauer who utilized the LAPW method [10].

3.3. Optical properties

The optical spectrum of the dielectric function ($\epsilon = \epsilon_1 + i\epsilon_2$) was calculated in our attempt to understand the optical transitions in ferroelectric $BaTiO_3$. The imaginary part of the dielectric function, ϵ_2, from the direct interband transitions, was calculated following equation (5) and using the calculated electronic wave functions and energies. The calculated real and imaginary parts of the dielectric function versus the photon energy are shown in figures 5(a) and 5(b). In figure 5, the solid lines represent the calculated results and the square symbols show the experimental data from Cardona [34]. From figure 5, we see that the calculated dielectric functions are in a good agreement with the experimental measurements [34]. The calculated optical spectra shown in figure 5 only include the direct interband transitions. The phonon-assisted indirect transitions will give a higher-order correction to the calculated optical spectrum.

The fundamental absorption edge E_0, which is also a measure of the direct optical gap, was found to be 3.2 eV from the calculation. This is the same as the experimental value [34]. Both of the experimental results and our calculated one show that the direct optical gap is larger than the smallest indirect band gap. On the basis of this investigation and the comparison of the calculated results with the experimentally measured data (such as the values of the band gap and the effective mass, and the optical spectrum), we conclude that the electronic structure reported in figure 1 is reasonably reliable.

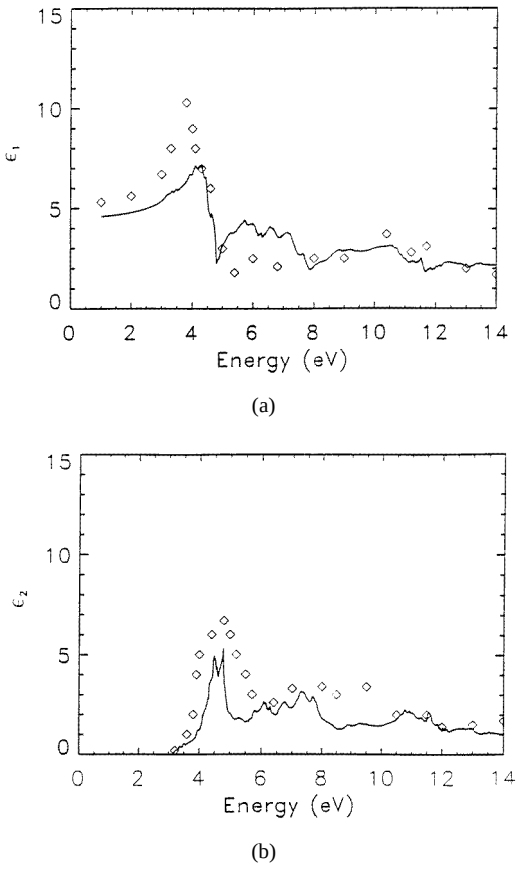

Figure 5. The optical spectrum of the dielectric function, $\epsilon = \epsilon_1 + i\epsilon_2$, as a function of the photon energy for ferroelectric $BaTiO_3$ in the tetragonal phase. (a) The real part, ϵ_1, of the dielectric function; and (b) the imaginary part, ϵ_2. The square symbols represent the experimental data.

4. Conclusion

We employed a local density potential, the LCAO method, and a new procedure to calculate the electronic structure, band gap, and optical properties of the ferroelectric tetragonal phase of $BaTiO_3$. It is shown that the band gap and low-energy conduction band can be predicted with a reasonable accuracy when the *ab initio* LCAO method is used with an optimum basis set of atomic orbitals. This basis set is selected to avoid a spurious effect inherently associated with any variational implementation of the LCAO method, where the charge density, in going from one iteration to the next, is constructed using only the wave functions for occupied states. The calculated effective mass for n-type carriers, the band gap, and the optical spectrum in ferroelectric tetragonal $BaTiO_3$ agree well with experimental results.

Acknowledgments

This work was supported in part by funding from the US DOE, through the Science and Engineering Alliance, under grant No DE-FG05-94ER25229, and the US Department of

the Navy, Office of Naval Research (ONR), under grant No N00014-96-1-0690, and grant No N00014-93-1-1368. The latter ONR award is to the Timbuktu Academy, directed by Dr Bagayoko.

References

[1] Lines M E and Glass A M 1977 *Principles and Applications of Ferroelectrics and Related Materials* (Oxford: Clarendon) ch 12
[2] Jaffe B, Cook W R and Jaffe H 1971 *Piezoelectric Ceramics* (New York: Academic) ch 5
[3] Zhang Q M, Zhao J, Shrout T, Kim N, Cross L E, Amin A and Kulwicki B M 1995 *J. Appl. Phys.* **77** 2549
[4] Cheng H F 1996 *J. Appl. Phys.* **79** 7965
[5] Hilton A D and Ricketts B W 1996 *J. Phys. D: Appl. Phys.* **29** 1321
[6] Schwartz R N, Wechsler B A and McFarlane R A 1992 *Phys. Rev.* B **46** 3263
[7] Michel-Calendini F M and Mesnard G 1973 *J. Phys. C: Solid State Phys.* **6** 1709
[8] Weyrich K H and Siems H 1985 *Z. Phys.* B **61** 63
[9] Mattheiss L F 1972 *Phys. Rev.* B **6** 4718
[10] Cohen R and Krakauer H 1992 *Ferroelectrics* **136** 65
[11] Cohen R and Krakauer H 1993 *Ferroelectrics* **150** 1
[12] Cohen R E and Krakauer H 1990 *Phys. Rev.* B **42** 6416
[13] Zhong W, Vanderbilt D and Rabe K M 1994 *Phys. Rev. Lett.* **73** 1861
[14] King-Smith R D and Vanderbilt D 1994 *Phys. Rev.* B **49** 5828
[15] Zhong W, King-Smith R D and Vanderbilt D 1994 *Phys. Rev. Lett.* **72** 3618
[16] Ghosez Ph, Gonze X, Lambin Ph and Michenaud J P 1995 *Phys. Rev.* B **51** 6765
[17] Ching W Y, Gu Z Q and Xu Y N 1994 *Phys. Rev.* B **50** 1992
[18] Sham L J and Schlüter M 1985 *Phys. Rev. Lett.* **51** 1418
Sham L J and Schlüter M 1985 *Phys. Rev.* B **32** 3883
[19] Hybertsen M S and Louie S G 1985 *Phys. Rev. Lett.* **55** 1418
Hybertsen M S and Louie S G 1986 *Phys. Rev.* B **34** 5390
[20] Zhu X and Louie S G 1986 *Phys. Rev. Lett.* **56** 2415
[21] Hohenberg P and Kohn W 1964 *Phys. Rev.* **136** B864
[22] Kohn W and Sham L J 1965 *Phys. Rev.* **140** A1133
[23] Vosko S H, Wilk L and Nusair M 1980 *Can. J. Phys.* **58** 1200
[24] Feibelman P J, Appelbaum J A and Hamann D R 1979 *Phys. Rev.* B **20** 1433
[25] Harmon B N, Weber W and Hamann D R 1982 *Phys. Rev.* B **25** 1109
[26] Zhao G L, Leung T C, Harmon B N, Keil M, Muller M and Weber W 1989 *Phys. Rev.* B **40** 7999
[27] Zhao G L and Harmon B N 1992 *Phys. Rev.* B **45** 2818
[28] Ching W Y, Xu Y, Zhao G L, Wong K W and Zandiehnadem F 1987 *Phys. Rev. Lett.* **59** 1333
[29] Ching W Y 1990 *J. Am. Ceram. Soc.* **73** 3135
[30] Evans H T 1961 *Acta Crystallogr.* **14** 1019
[31] Megaw H D 1962 *Acta Crystallogr.* **15** 972
[32] Mahgerefteh D, Kirillov D, Cudney R S, Bacher G D, Pierce R M and Feinberg J 1996 *Phys. Rev.* B **53** 7094
[33] Berglund C N and Baer W S 1967 *Phys. Rev.* **157** 358
[34] Cardona M 1965 *Phys. Rev.* **140** A651